Airborne Observations of a Catalina Eddy

THOMAS R. PARISH

Department of Atmospheric Science, University of Wyoming, Laramie, Wyoming

DAVID A. RAHN

Atmospheric Science Program, Department of Geography, University of Kansas, Lawrence, Kansas

DAVE LEON

Department of Atmospheric Science, University of Wyoming, Laramie, Wyoming

(Manuscript received 16 January 2013, in final form 10 April 2013)

ABSTRACT

Summertime low-level winds over the ocean adjacent to the California coast are typically from the north, roughly parallel to the coastline. Past Point Conception the flow often turns eastward, thereby generating cyclonic vorticity in the California Bight. Clouds are frequently present when the cyclonic motion is well developed and at such times the circulation is referred to as a Catalina eddy. Onshore flow south of the California Bight associated with the eddy circulation can result in a thickening of the low-level marine stratus adjacent to the coast. During nighttime hours the marine stratus typically expands over a larger area and moves northward along the coast with the cyclonic circulation. A Catalina eddy was captured during the Precision Atmospheric Marine Boundary Layer Experiment in June of 2012. Measurements were made of the cloud structure in the marine layer and the horizontal pressure field associated with the cyclonic circulation using the University of Wyoming King Air research aircraft. Airborne measurements show that the coastal mountains to the south of Los Angeles block the flow, resulting in enhanced marine stratus heights and a local pressure maximum near the coast. The horizontal pressure field also supports a south–north movement of marine stratus. Little evidence of leeside troughing south of Santa Barbara, California, was observed for this case, implying that the horizontal pressure field is forced primarily through topographic blocking by the coastal terrain south of Los Angeles, California, and the ambient large-scale circulation associated with the mean flow.

1. Introduction

Time-averaged low-level flow in the summertime marine boundary layer (MBL) off the California coast is the result of the broad Pacific high situated several hundred kilometers to the west of the coast and the persistent thermal low over the desert southwest. As a consequence, summertime winds in the MBL along the U.S. West Coast are typically from the north and tend to be parallel to the coastline. An extensive body of literature examines the role of the coastal terrain on the MBL flow (e.g., Dorman 1985; Beardsley et al. 1987; Zemba and Friehe 1987; Mass and Albright 1987; Burk and Thompson 1996; Nuss et al. 2000; Pomeroy and Parish 2001; Koračin and Dorman 2001; Rahn and Parish 2007). As noted in Dorman and Koračin (2008), Point Conception (see Fig. 1) is the most extreme bend in the western U.S. coastline and pronounced changes in low-level wind speed and direction occur near this point. As the northerly flow impinges on the elevated topography of the coastal range to the north of Point Conception, significant deceleration occurs and a compression bulge has been suggested. To the east of Point Conception, the surface wind decreases in speed and the mean direction of the summertime marine layer flow becomes more westerly (e.g., Dorman and Winant 2000). Cyclonic vorticity is thus commonplace in the California Bight, especially during summer.

As an example of the mean early summer climatology, Fig. 2 illustrates the 2008 June monthly-mean 1000-hPa heights, wind speeds, and streamlines within the California

Corresponding author address: Thomas R. Parish, Department of Atmospheric Science, University of Wyoming, Laramie, WY 82071.
E-mail: parish@uwyo.edu

DOI: 10.1175/MWR-D-13-00029.1

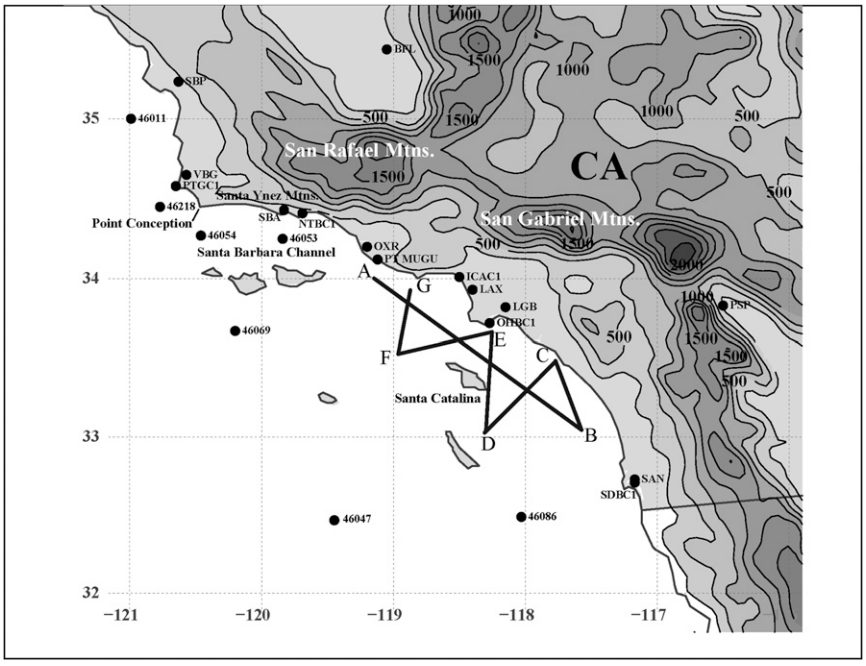

FIG. 1. Key stations, buoys, and geographical features in California Bight area. Terrain contours in meters with darkest shading indicating highest elevations. PreAMBLE flight track of the UWKA for 9 Jun 2012 case indicated by labeled bold line.

Bight from the operational National Centers for Environmental Prediction (NCEP) ~5-km High-Resolution Window Forecast System (HIRESW). A sharp gradient in the 1000-hPa wind speed exists across the California Bight and wind speeds decrease to the east. Streamlines of the 1000-hPa wind show a directional shift from predominantly northerly winds west of Point Conception to a more westerly component within the California Bight. The mean 1000-hPa level corresponds to a height above the ocean surface of about 100 m; note that the mean June 2008 height field along the eastern edge of the California Bight shows a weak north–south gradient with higher heights to the south. Analyses (not shown) indicate that cyclonic vorticity is a low-level feature of the California Bight region with a maximum near 1000 hPa and extending to about 900 hPa. Such mean wind conditions suggest that the formation of low-level cyclonic eddies in the marine layer of the bight region is a climatological norm and thus no special atmospheric circumstances are required to initiate cyclonic vorticity during the early summer period.

Catalina eddies represent an enhanced cyclonic circulation in the California Bight and have attracted considerable attention since publication of the satellite image by Rosenthal (1968). A typical pattern consists of cyclonic circulation centered in the California Bight region near Santa Catalina Island with a strong diurnal variation in marine stratus thickness and spatial extent. These circulations are most common during the early summer months (Mass and Albright 1989). Catalina eddies are known for their extensive low stratus coverage along the eastern half of the California Bight, often deepening near the coast and extending inland through mountain passes. Cloud coverage is especially enhanced during the nighttime hours. As with coastally trapped wind reversals, longwave radiational cooling at cloud top effectively cools the entire marine layer (e.g., Thompson et al. 1997; Rahn and Parish 2008) and the stratus can expand spatially and surge northward. Insolation tends to dissipate the marine stratus and the northward progression of the leading edge of the clouds associated with the eddy can slow during daytime hours. During well-developed Catalina eddies, the typical Southern California pattern of marine stratus dissipation in morning or the early afternoon hours is delayed. Temperatures near the coast can be more than 5°C below normal if the marine stratus persists for much of the day (e.g., Wakimoto 1987).

Low-level flow along the coast from Baja California to Los Angeles, California, often develops a southerly component in response to the cyclonic circulation. Such flows are well known to the local surfing community as being a bane to favorable ocean conditions. Bosart (1983) was among the first to study the eddy circulation and listed several factors that have been attributed to its formation including leeside troughing associated with

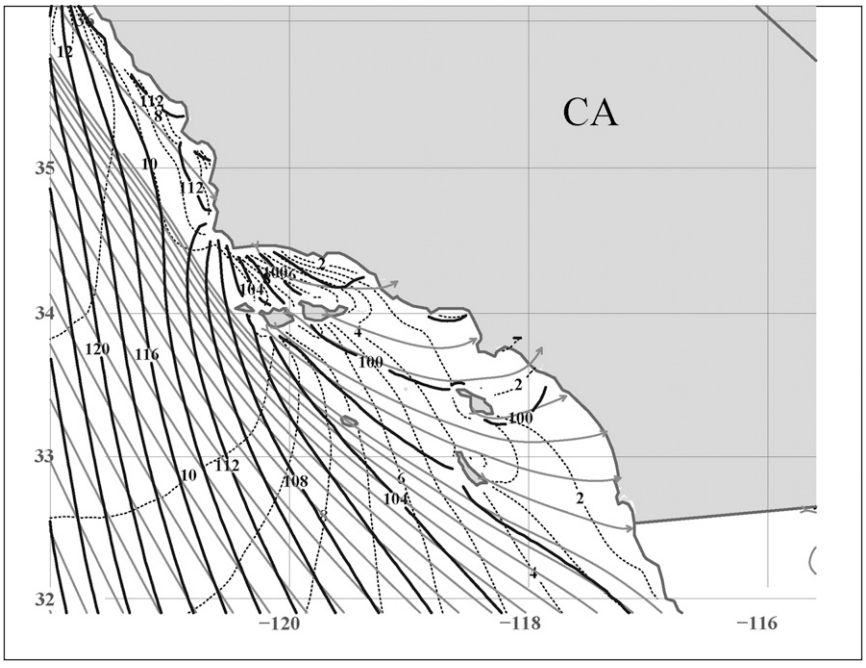

FIG. 2. Mean June 2008 1000-hPa field of height contours (thick line, m), wind speeds (dashed lines, m s^{-1}), and streamlines (gray solid lines) based on NCEP High-Resolution Window Forecast System.

the San Rafael and Santa Ynez mountains between Point Conception and Point Mugu, California. Wakimoto (1987) suggests that the eddy circulation is an example of a mechanically forced vortex as air flows around Point Conception. He also notes that the increased depth of the mixed layer accompanying a Catalina eddy helps improve air quality in the greater Los Angeles area. Mass and Albright (1989) conducted a comprehensive survey of 50 Catalina eddy events to determine the origin of cyclonic circulation. Their analyses suggest that an 850-hPa trough extending southwest over the Southern California region enhances the horizontal pressure field in the marine environment, thereby intensifying the northerly flow along the California coast to the north of Point Conception. Similar to Bosart (1983), they conclude that the lee troughing in response to flow over the San Rafael and Santa Ynez mountains forces a local pressure gradient with higher pressure to the south within the California Bight. According to Mass and Albright (1987), thickening of the marine stratus deck is the result of blocking by the coastal mountains similar to damming of cold air against topography as originally proposed by Schwerdtfeger (1975). Southerly flows similar to barrier winds then develop within a Rossby radius of deformation from the coastal mountains. Clark and Dembek (1991) examined a Catalina eddy case from 1987, noting again the role of enhanced northerly flow over the coastal mountains east of Point Conception in the development of a leeside trough.

Numerical simulations by Ueyoshi and Roads (1993) were among the first of a Catalina eddy, focusing on the same 26–30 June 1988 Catalina eddy event discussed by Mass and Albright (1989). Their results suggested that downslope wind from the mountains to the east of Point Conception resulted in warm air over the Channel Islands that helped create and maintain the horizontal pressure field associated with the Catalina eddy. Ulrickson et al. (1995) also conducted numerical simulations of the same Catalina eddy event. They note that the eddy circulation is forced by a combination of cyclonic turning of the northwest flow north of Point Conception to more westerly in the Santa Barbara Channel and forcing of the southerly flow in the near-coastal marine environment as a result of the mountains to the south of Los Angeles. Davis et al. (2000) also examined that same Catalina eddy case, concluding that synoptic-scale enhanced flow over the San Rafael and Santa Ynez mountains results in leeside vorticity generation. Model results also suggest two scales of response to flow over the mountains including a mountain wave feature and the broad mesoscale warm air pool that encompasses much of the eddy circulation. The authors note the importance of the strength of the northerly low-level wind field and that an optimal speed

is necessary for the eddy circulation to remain in the California Bight.

Modeling work was also extended by Thompson et al. (1997) who simulated the Catalina eddy case from 21 July 1992. They note that as in previous studies the Catalina eddy forms in response to intensification of the horizontal pressure gradient (PGF) along the California coast to the north of Point Conception that helps drive northwesterly flow over the mountains to the east of Point Conception that results in lee troughing and higher pressure to the south of the California Bight. Model results indicate that the coastal mountains to the south of Los Angeles are responsible for deepening of the MBL through blocking and that the radiation budget of the clouds is critical for boundary layer thermodynamics within the eddy circulation. Finally, Skamarock et al. (2002) also point to the role of lee troughing in producing the eddy circulation and offer that the dynamics of the Catalina eddy are similar to those at work in coastally trapped wind reversals (e.g., Nuss et al. 2000; Parish et al. 2008; Rahn and Parish 2008).

Here airborne observations made by the University of Wyoming King Air research aircraft (UWKA) of a Catalina eddy circulation are presented. Data were collected as part of the Precision Atmospheric Marine Boundary Layer Experiment (PreAMBLE) and observations discussed here are taken from the eddy circulation observed on 9 June 2012. The purpose of the paper is to present evidence as to the dynamics that force the eddy circulation in the California Bight region. Stimulus for the study was the acknowledged lack of observations of key meteorological processes in the MBL near Point Conception (i.e., Davis et al. 2000; Skamarock et al. 2002) that have limited verification of key results from numerical studies.

2. PreAMBLE airborne measurements

PreAMBLE was a field study conducted from mid-May to mid-June 2012 based in Point Mugu, California, with the central purpose of examining in detail the atmospheric dynamics associated with the summertime MBL near Point Conception and the California Bight area using an airborne measurement platform. In particular, the ability of the UWKA to map the horizontal pressure field is exploited. To understand the dynamics of atmospheric motions, it is imperative that proper measurement of the horizontal pressure gradient force (PGF) be made. UWKA flight legs are often conducted along isobaric surfaces; the slope of an isobaric surface is directly proportional to the PGF. Thus, the critical measurement is the height of the isobaric surface above some reference such as sea level. Radar altimeters have been used in the past to independently measure aircraft height, yet the measurement becomes compromised over irregular terrain or even over the ocean during periods of large swell. Since horizontal pressure fluctuations of about 0.1 hPa can be significant, the height of the measurement platform must be known to within a fraction of a meter. This accuracy has been achieved using differential GPS processing of UWKA data (e.g., Parish et al. 2007; Parish and Leon 2013).

Differential GPS measurements require deployment of one or more reference GPS stations. The position of this reference GPS receiver is known to a high degree of precision that is then used to correct the position of the GPS data collected by the UWKA platform. During PreAMBLE, a GPS base station receiver was deployed near the hangar which housed the UWKA at Point Mugu, California. Base station GPS data were recorded at 10 Hz for the duration of the project. When combined with an accurate static pressure measurement, the PGF can be calculated. As noted in Parish et al. (2007) and Parish and Leon (2013), small deviations of the aircraft autopilot off the isobaric surface are inevitable and have been corrected using the hypsometric equation. Details of the dGPS technique, sources of error and limitations to the measurement accuracy are given in Parish et al. (2007) and Parish and Leon (2013). All isobaric heights shown are with respect to mean sea level.

One recurring issue in determining the PGF is the correct transformation between space and time. A normal flight leg can be 50 km or more, requiring 10 min or so of flight time. To accurately assess the horizontal pressure field it is essential that pressure tendency is considered. Reciprocal legs (back and forth along the same flight track) have been used in the past to resolve this issue when interpreting pressure information along legs. When there are reciprocal flight legs, the effect of the changing pressure field can be removed by interpolating to a single isobaric height. The height difference between the legs can then be used to infer a mean height change of the isobaric surface during the course of the reciprocal legs. At times it is not feasible to conduct these repeating legs, so other information is required to correct for the pressure tendency. As part of this Catalina eddy study, flight legs were conducted mostly within the lowest few hundred meters above the ocean. The UWKA was used to measure the PGF in both the alongshore and cross-shore directions south of Los Angeles. An extensive array of buoys is deployed about the California Bight (some shown in Fig. 1) that can help with determination of isallobaric tendencies at particular locations.

During PreAMBLE the UWKA carried both upward- and downward-looking versions of the Wyoming Cloud lidar (WCL). The WCL is a 355-nm lidar designed for

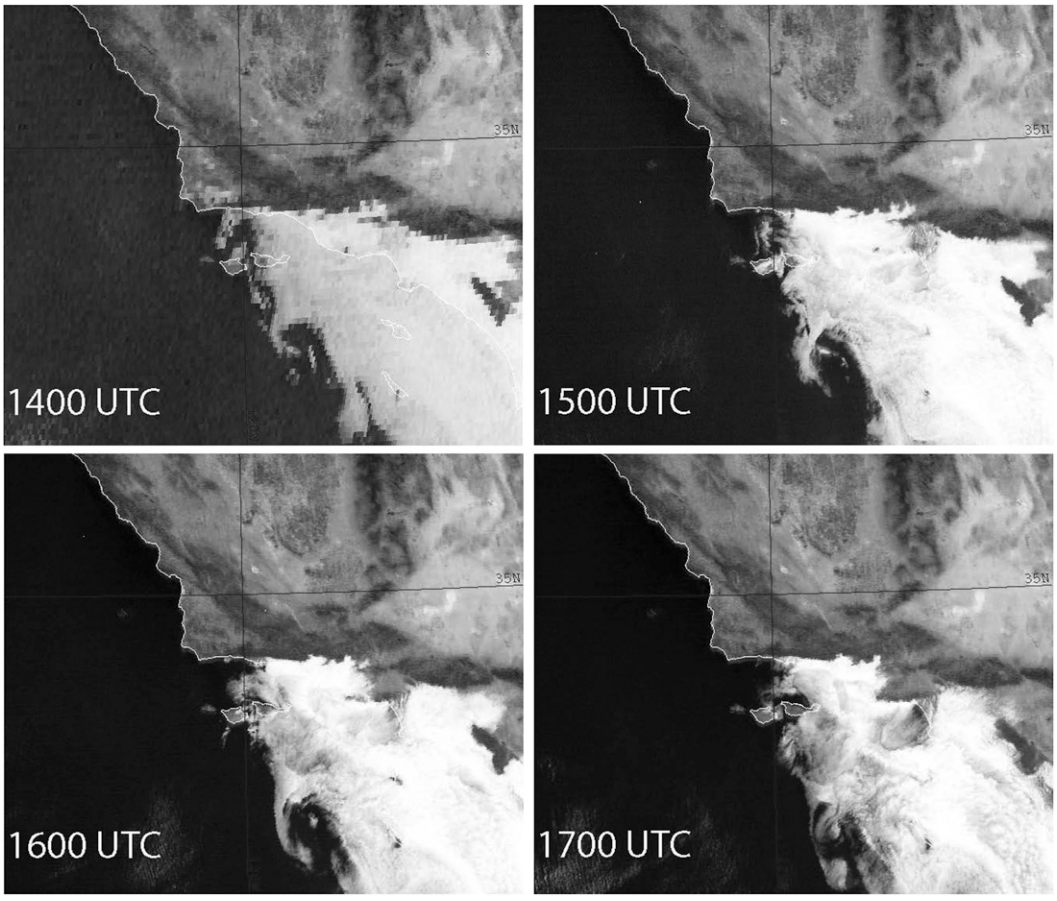

FIG. 3. GOES-West visible imagery over California Bight region during time of UWKA mission from 1400 to 1700 UTC 9 Jun 2012.

retrieval of cloud and aerosol properties. The returned signal for the upward-looking lidar is sampled at 3.75-m intervals, while the returned signal for the downward-looking lidar is sampled at 1.5-m intervals. Additional details of the upward- and downward-looking WCLs can be found in Wang et al. (2009) and Wang et al. (2012). The lidar data are combined with INS/GPS data from the UWKA to produce time–height images of the (uncalibrated) attenuated backscatter. The lidars are well suited to determine of cloud boundaries, but because the lidar signal is rapidly attenuated in cloud, the lidars are unable to penetrate deeply into the cloud layer.

3. Results

a. Discussion

Figure 3 illustrates the Geostationary Operational Environmental Satellite-West (GOES-West) visible images of the California Bight on 9 June 2012 during the period of the UWKA mission. Extensive marine stratus is present over the eastern half of the California Bight and a classic hook structure is present in the cloud layer west of San Clemente Island, showing the cyclonic circulation. Winds from the south near San Diego, California, are often indicative of a Catalina eddy (Mass and Albright 1989). Data from buoy 46086 (see Fig. 1) situated just west of San Diego indicated a wind of $\sim 4\,\mathrm{m\,s^{-1}}$ from 170° at 1500 UTC. Southerly flow persisted at this site until late afternoon. A cyclonic circulation was apparent during the early morning hours on the previous day and the two days following the event described here. Typically, the cyclonic circulation develops during the nighttime hours and, in terms of stratus coverage, is best developed near sunrise. Satellite imagery for each day (not shown) depicted northward movement of the stratus near the coast during the early morning hours, turning to a more easterly direction near Point Mugu. Stratus coverage and inferred eddy circulation decreased during the afternoon hours.

At the time of the flight, an upper-level trough was over the Rocky Mountains as shown from the 0.5° by

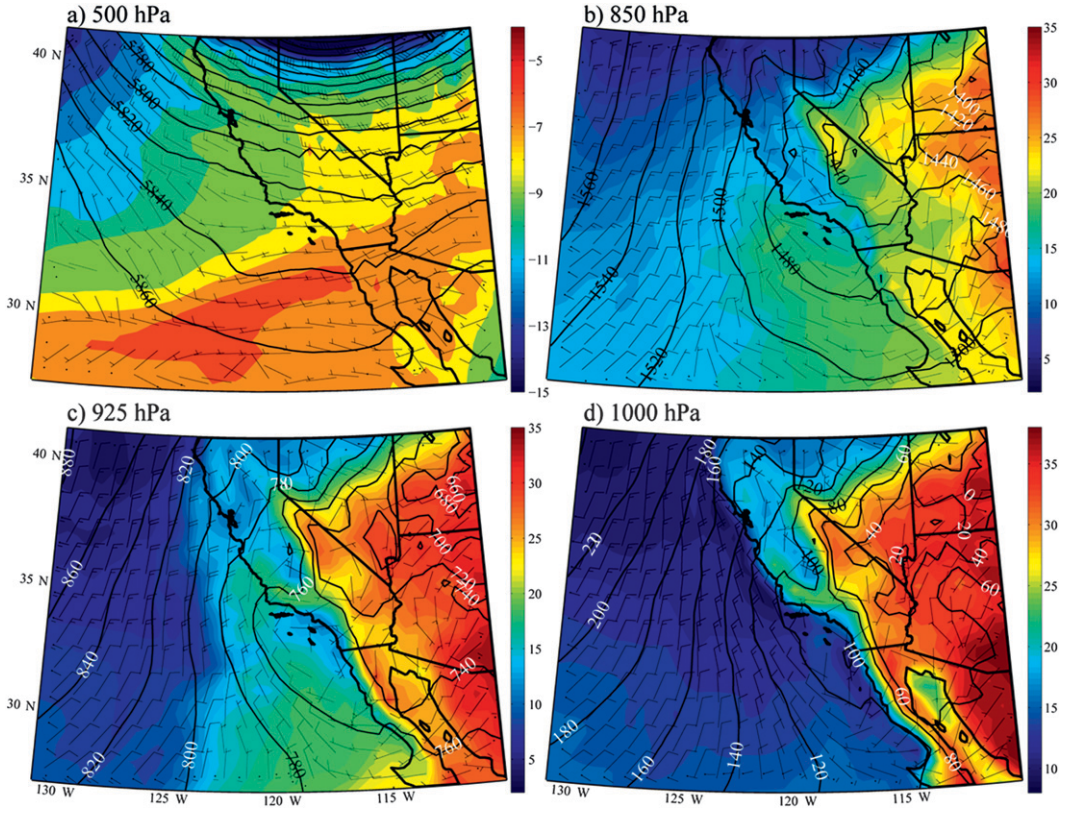

FIG. 4. Geopotential height (m, contours), temperature (°C, color), and wind barbs (m s^{-1}) at 1200 UTC 9 Jun 2012 at (a) 500, (b) 850, (c) 925, and (d) 1000 hPa from the Climate Forecast System Reanalysis.

0.5° grid NCEP Climate Forecast System Reanalysis in Fig. 4 (Saha et al. 2010). Associated with this trough were midlevel (500 hPa) winds from between west-southwest and west-northwest over the California Bight, while closer to the surface the wind direction becomes more northwesterly, reflecting the surface anticyclone. Southwesterly (onshore) flow is present over Baja from at 850 hPa; below 850 hPa, the onshore flow weakens but is still present. The diminishing onshore flow toward the surface is likely tied to the topography. Blocking and a deeper MBL are apparent even in the relatively coarse model domain. At 925 hPa (about 800 m) a band of cooler temperatures is found along the Southern California coast, indicative of the marine air piling up along the coast. Features of the MBL response to the onshore flow are revealed in detail by the aircraft measurements.

The flight pattern used on 9 June 2012, shown in Fig. 1, was designed to document both the coast-parallel pressure gradient and also the pressure gradient and atmospheric structure normal to the coastline. The flight started with a climbout sounding to about 1000 m, followed by a long, coast-parallel isobaric leg (A-B) at 994 hPa, (~150 m above the ocean surface). The UWKA then conducted a series of legs normal to the coastline (C–D). This set consisted of a pair of reciprocal, isobaric legs at 994 hPa followed by a reciprocal pair of sawtooth legs between ~200 and ~900 m (again C–D). A single leg from C–D at ~900 m was then conducted so the WCL could track cloud top height. The UWKA then headed due north (D–E) on the 994-hPa isobaric surface, before conducting another set of legs normal to the coastline (E–F). This set consisted, again, of a pair of reciprocal, isobaric legs at 994 hPa, this time followed by a single sawtooth leg. This set was followed by a final isobaric leg at 994 hPa (F–G) on a northward heading.

b. *Alongshore features*

The UWKA departed the airport at Point Mugu at 1406 UTC 9 June 2012 heading south. As the aircraft climbed after takeoff, the depth and thermodynamic structure of the MBL was captured just offshore (Fig. 5). The UWKA reached the coastline when it was about 200 m above the surface. Clouds were encountered in the coastal environment with a base of ~650 m and tops of ~770 m. As is typical for summertime marine stratocumulus in this region, the cloud top corresponds to the top of the MBL as indicated in the sounding data shown in Fig. 5. Potential temperatures (Fig. 5a) indicate

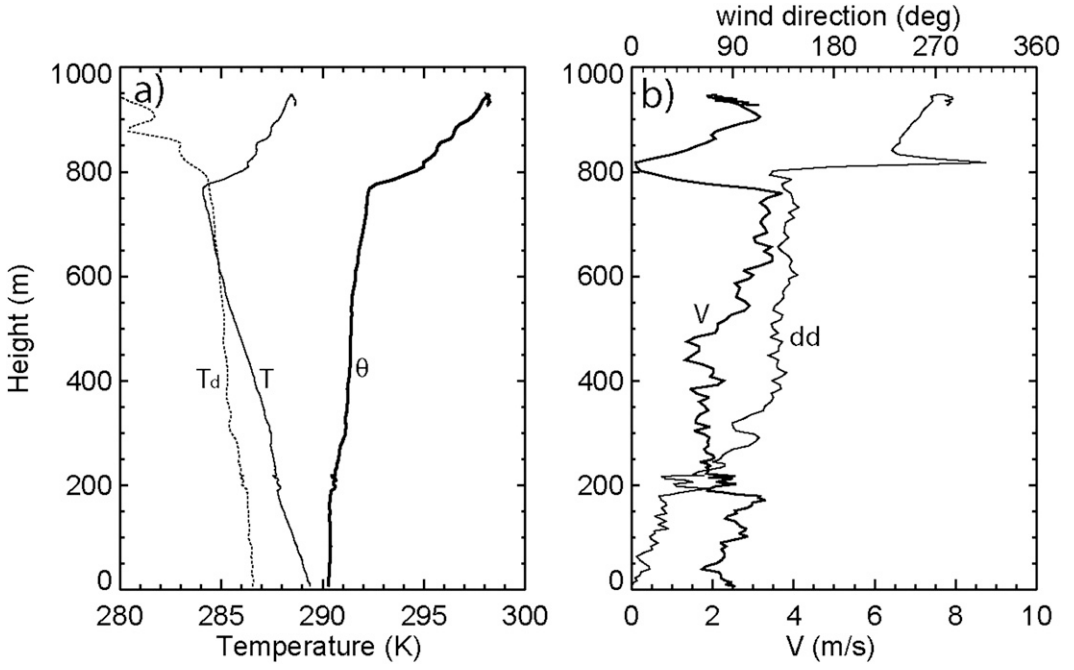

FIG. 5. Climb-out sounding conducted by UWKA at 1406–1410 UTC 9 Jun 2012. (a) Potential temperature (thick, solid line, K), temperature (thin, solid line, K), and dewpoint temperature (dashed line, K); (b) wind speed (thick, solid line, m s^{-1}) and wind direction (thin, solid line, degrees).

a fairly well-mixed boundary layer from the surface to 770 m with the classic signature of a subsidence inversion as indicated by temperature and dewpoint profiles above 770 m. Cloud layer observations are consistent with UWKA measurements of temperature and dewpoint. Once the UWKA was over the ocean, winds were only about 2 m s^{-1} from directions 90° to 120°, roughly following the regional coastline. Thus, the eastern branch of the Catalina eddy circulation and associated stratus could be observed just offshore from Point Mugu.

After the initial ascent, the UWKA began an isobaric leg 150 m above the ocean heading southeast from A to B in Fig. 1, which is roughly parallel to the coast. The purpose of the leg was to map the horizontal pressure field in a north–south direction along the coast associated with the Catalina eddy circulation. Satellite imagery during PreAMBLE frequently showed northward movement of the stratus during the nighttime and early morning hours, consistent with a northward-directed PGF and hence isobaric height increases to the south. Figure 6 illustrates UWKA measurements along the track. Corrected heights of the 994-hPa surface (Fig. 6a) increase to the south by about 2 m over the approximately 150-km leg. This corresponds to a geostrophic wind of 1.6 m s^{-1} normal to the leg. Wind speed along the flight leg (Fig. 6b) is fairly uniform at 3–4 m s^{-1}. Wind directions averaged over the entire leg are from 127°, nearly the same as the track angle of 125° implying a negligible wind component across the leg. A shift is seen in wind directions from a predominant easterly direction at the start of the leg to a more southerly component south of the Long Beach, California, area. This corresponds well with the regional terrain and reflects the cyclonic circulation depicted in the satellite imagery (e.g., Fig. 3). From this analysis the observed winds display downgradient acceleration with respect to the pressure field. Temperatures (Fig. 5c) along the isobaric leg decrease southward by about 2°C, again consistent with blocking of the flow to the south (e.g., Schwerdtfeger 1975). Dewpoint temperatures remain roughly constant along the leg.

Such observations support the findings of Mass and Albright (1989) in that the winds associated with the Catalina eddy are ageostrophic in the alongshore direction, propagating northward in response to a favorable pressure field. Observations on this day, however, do not support extensive leeside troughing in the Santa Barbara Channel. As seen in the time-averaged map (Fig. 2), the alongshore pressure gradient such as indicated in Fig. 6a can occur without the need for strong leeside troughing since the continent itself is characterized by pressures lower than those seen over the ocean. In addition, the blocking of the flow to the south of Los Angeles by the coastal mountains can enhance pressures

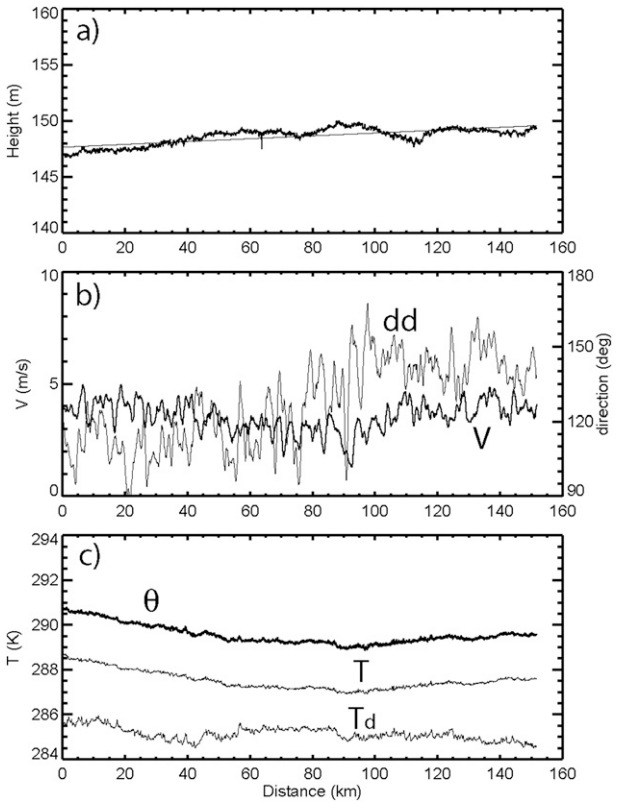

FIG. 6. UWKA measurements from 994-hPa leg A–B at 1414–1447 UTC 9 Jun 2012 of (a) heights (bold line, m) and least squares linear fit (thin, solid line); (b) wind speed (bold line, $m\,s^{-1}$) and wind direction (thin line, degrees); and (c) potential temperature (bold, solid line, K), temperature (thin, solid line, K), and dewpoint temperature (dashed line, K). North is to left.

to the south (e.g., Mass and Albright 1989; Thompson et al. 1997) and thereby intensify existing alongshore horizontal pressure gradients.

Data from coastal buoys also support the lack of lee-side troughing. Surface measurements of pressure and wind are available at buoys (moving clockwise from the north) PTGC1 near Vandenberg, 46054 south of Point Conception, 46053 south of Santa Barbara within the Santa Barbara Channel, NTBC1 near Santa Barbara, ICAC1 at Santa Monica, OHBC1 near Long Beach, SDBC1 at San Diego 46086 southeast of San Diego, and 46047 situated south of San Clemente Island (see Fig. 1). Buoys PTGC1 and 46054 reported strong northwest winds from 12 to 15 $m\,s^{-1}$ throughout the morning hours of 9 June. Buoy 46054 at the western end of the Santa Barbara Channel indicated winds from 325°, fully exposed to flow from out over the ocean. Key buoys with respect to effects of downslope flow off Santa Ynez and San Rafael mountains were 46053 and NTBC1. Winds at 46053 buoys were weak (less than 5 $m\,s^{-1}$) with variable wind directions that at the 1400 UTC take-off time were from 210°. Buoy 46053 situated closer to shore also experienced weak winds with variable wind direction. No evidence of sustained northerly winds was seen for either site during the previous nighttime or early morning hours on 9 June.

Evidence from the satellite imagery indicated that the clouds associated with the Catalina eddy circulation did not extend westward past Santa Barbara. This is consistent with the pressure measurements at buoys within the California Bight region. At 1400 UTC, buoy NTBC1 had a pressure of 1011.2 hPa while buoy ICAC1 situated about 100 km to the east reported a surface pressure of 1010.5 hPa and buoy OHBC1 some 30 km farther east indicated a pressure of 1010.3 hPa. Pressures thus indicate a monotonic pressure decrease along the coast from Point Conception to just south of Los Angeles during the time of UWKA observations. Pressure decreases to the east along the coast from Santa Barbara to at least Long Beach, consistent with the movement of the cloud surge from the Catalina eddy that never reaches Santa Barbara owing to an adverse PGF in the Santa Barbara Channel. To the south of Los Angeles pressures again rise, consistent with the impinging of the flow against the coastal mountains and blocking conditions as suggested by Mass and Albright (1989) and Thompson et al. (1997). No evidence of significant lee-side troughing within the Santa Barbara Channel exists for this case and it is concluded that the origin of the Catalina eddy is not tied to downsloping flow off the Santa Ynez or San Rafael ranges.

c. *Cross-shore measurements*

Variation of pressure in a direction normal to the coast along the section of coastline south of Los Angeles was evaluated by reciprocal legs between points C and D as shown in Fig. 1. Flight level was about 150 m above the ocean. Effects of blocking on the Catalina eddy have been established by, for example, Mass and Albright (1989) and Thompson et al. (1997). For the case shown, surface pressures were rising throughout the California Bight and isobaric heights were corrected for this regional change that is part of a semidiurnal oscillation (e.g., Mass and Albright 1989). Figure 7 illustrates results from two UWKA legs conducted normal to the coast. Effects of blocking are apparent with heights approximately 1.5 m higher near the coast (Fig. 7a), corresponding to a pressure difference of 0.2 hPa. Winds along these legs (Fig. 7b) are predominantly coast parallel with a mean speed of 3.6 $m\,s^{-1}$. From the isobaric slope in Fig. 7a, the geostrophic wind normal to the leg and parallel to the coast amounts to 2.9 $m\,s^{-1}$. Winds associated with the Catalina eddy can be classified as cyclonic. A radius of curvature of ~150 km is estimated

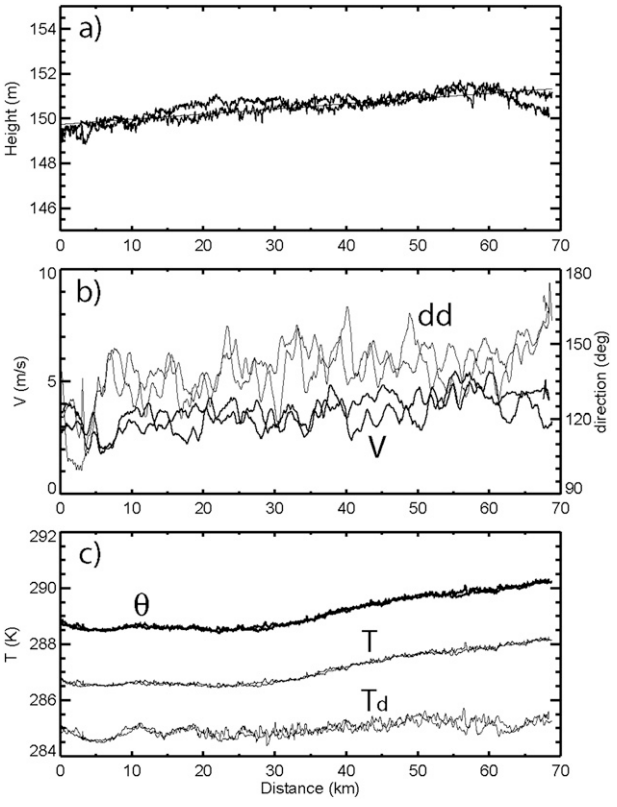

FIG. 7. As in Fig. 6, but for leg C–D 1527–1557 UTC. East is to right.

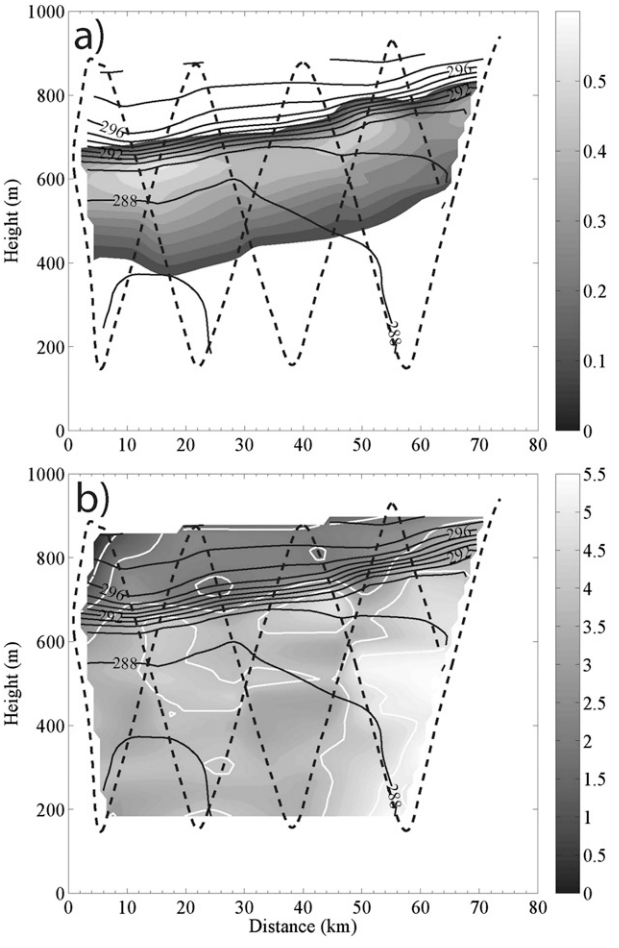

FIG. 8. UWKA measurements during sawtooth profiling along leg C–D at 1526–1557 UTC 9 Jun 2012 showing (a) isentropes (dark, thick lines; K) and liquid water content (shading; g m^{-3}) and (b) isentropes and coast-parallel component of wind (shading; m s^{-1}). UWKA track depicted by dashed lines. East is to right.

from satellite imagery. The gradient wind speed of cyclonic flow, which by definition is subgeostrophic, is approximately 2.4 m s^{-1}. It is concluded from such calculations that the observed coast-parallel wind exceeds the expected gradient wind by about 50% and is supergeostrophic by somewhat less than 1 m s^{-1}. Taking into account any frictional effects reinforces this conclusion. A picture emerges that suggests blocking is occurring but the flow is supergeostrophic in response to an along-coast horizontal pressure gradient force component pointing north that is accelerating the flow as seen by measurements along leg A–B. Temperatures (Fig. 7c) near the coast are warmer than those found offshore by about 2°C, no doubt tied to sea surface temperatures (not shown) that show similar trends.

To examine the vertical structure normal to the coast, sawtooth maneuvers were performed along the same cross-shore track between points C and D in Fig. 1. Ascent and descent rates were limited to 250 m min^{-1} to ensure accurate wind determination from the airborne platform. This implied that time required for the UWKA to conduct soundings from roughly 100 to 900 m corresponds to a horizontal distance of about 18 km. To sample the atmosphere efficiently, the reciprocal sawtooth leg was conducted in a manner such that its ascent portions corresponded with descent portion from the previous leg. Figure 8a illustrates a cross section constructed from the reciprocal sawtooth legs of potential temperature and cloud liquid water as inferred from the Droplet Measurement Technologies Hot-Wire Liquid Water Sensor (LWC-100) probe on the UWKA. Cloud boundaries are defined by a liquid water content >0.10 g m^{-3}. Effects of blocking are evident in the potential temperature surfaces that rise by approximately 150 m from west to east along the 75-km leg. From hydrostatic considerations, the enhanced depth of the MBL near the coast is consistent with the pressure increase observed from the UWKA. Marine stratus associated with the Catalina eddy is roughly of uniform thickness across the leg but follows the trend in potential temperatures such that both cloud base and cloud top are roughly 150 m higher

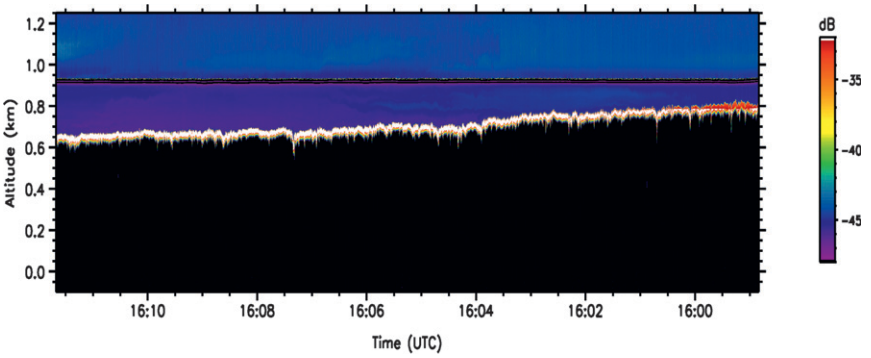

FIG. 9. Attenuated backscatter (uncalibrated, dB) from University of Wyoming Cloud lidar along leg C–D at 1559–1611 UTC 9 Jun 2012 illustrating cloud-top height (m). East is to right.

at the east end of the leg. Cloud tops are tied to the temperature inversion at the top of the MBL. The eastward increase in the base of the marine stratus is due to the approximately 2°C warmer sea surface temperatures found at the coast.

Winds in the MBL as observed from the UWKA during the sawtooth profiles are directed primarily along the coastline with a mean direction of about 130°. Wind speeds of the coast-parallel component are generally less than $5\,m\,s^{-1}$ (Fig. 8b) with a slight enhancement toward the coast. Above the marine inversion wind directions remained southeasterly below 1000 m but wind speeds decreased above the inversion to less than $2\,m\,s^{-1}$.

An additional leg along CD was flown above the cloud-topped MBL to take advantage of the WCL. Using the downward-looking beam, a continuous measurement of the cloud-top height was obtained. The WCL may detect small-scale variations of the cloud-top height and any features that the individual soundings through the top of the MBL might miss. Figure 9 illustrates the variation of the cloud-top height along the leg as determined from the WCL. The slope of the cloud top is similar to that illustrated in Fig. 8, confirming the interpolated in situ measurements from the UWKA that cloud tops range from about 800 m along the eastern end to about 625 m at the western edge of the approximately 70-km leg.

d. Returning legs

Following the vertical sawtooth leg, the UWKA headed nearly due north at an isobaric level of 994 hPa from points D to E in Fig. 1. Competing influences arising from effects of blocking by the coastal topography and the observed south–north pressure decrease complicate interpretation of the isobaric height surface along the track. Again, heights have been corrected based on the observed pressure tendency during the time of the leg at buoy OHBC1. Corrected heights (Fig. 10a) are greatest at the northern end of the leg. The isobaric slope supports a $2.0\,m\,s^{-1}$ easterly geostrophic wind that is in reasonable geostrophic balance with the observed mean $2.7\,m\,s^{-1}$ easterly component of the wind. Wind speeds and wind directions (Fig. 10b) are relatively uniform along the leg with a mean wind speed of $3.7\,m\,s^{-1}$ from 129°, roughly parallel to the coastline. As with leg C–D, it is concluded that winds associated with the cyclonic circulation are in excess of expected gradient winds

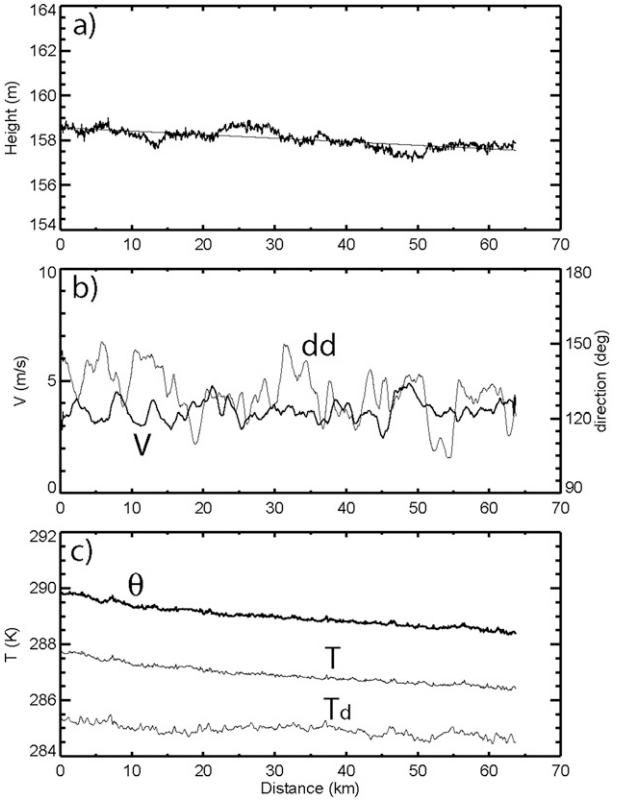

FIG. 10. As in Fig. 6, but for leg D–E at 1614–1627 UTC. North is to left.

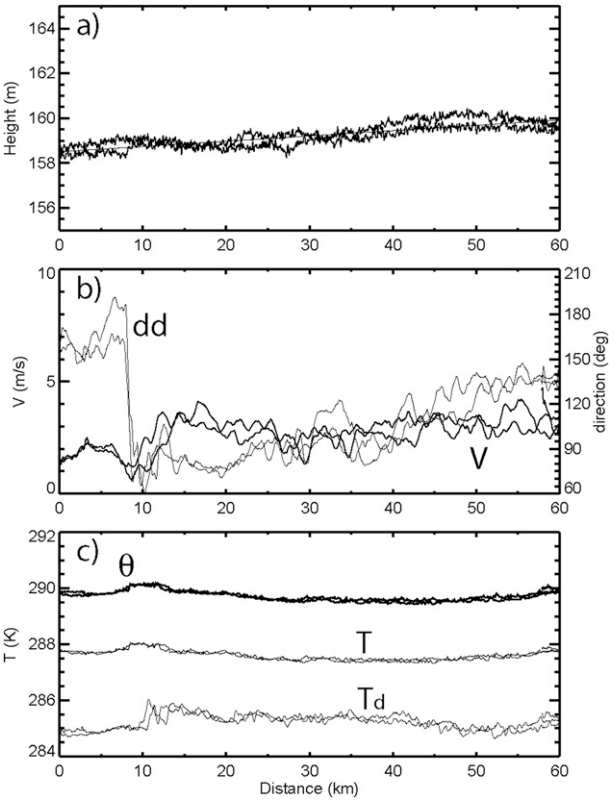

FIG. 11. As in Fig. 6, but for leg E–F at 1627–1653 UTC. East is to right.

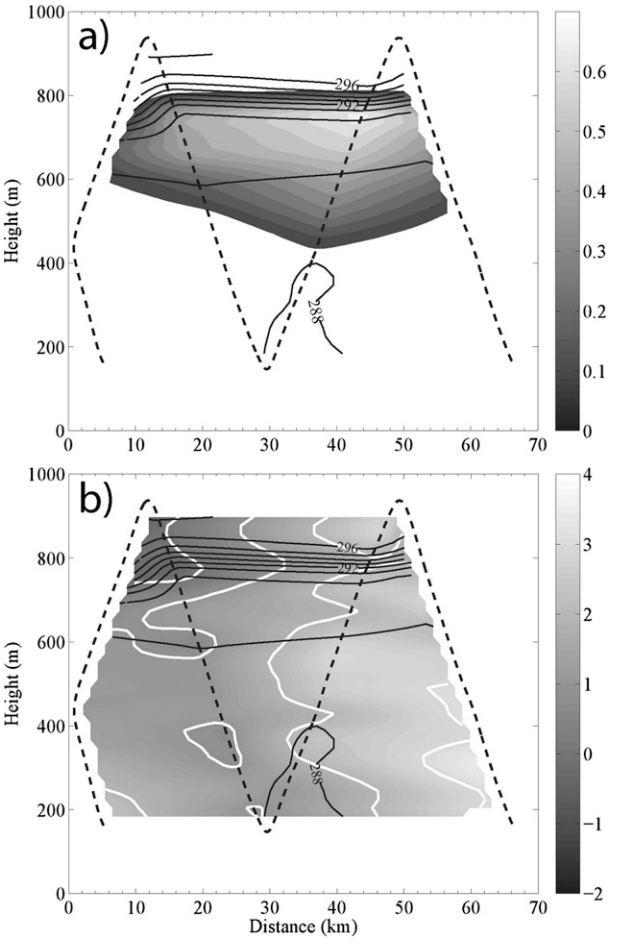

FIG. 12. As in Fig. 8, but along leg E–F at 1654–1705 UTC. East is to right.

and show evidence of tangential accelerations accompanying the mesoscale pressure field. Potential and actual temperatures at about 150 m above the ocean (Fig. 10c) increase toward the coast by about 1.5°C over the course of the leg although the dewpoints remain roughly constant.

Additional reciprocal isobaric legs at about 150 m above the ocean were then conducted along line E–F as shown in Fig. 1. Buoy data at OHBC1, ICAC1, and NTBC1 each show that the surface pressure field remained nearly constant during the time of this leg. Evaluation of the isobaric heights along leg EF confirmed this as each leg traced out essentially the same pattern. Figure 11 illustrates UWKA measurements from the reciprocal legs. Highest heights of the 994-hPa surface (Fig. 11a) are found at the east end of the leg and then drop by about 1.5 m over the 60-km leg, corresponding to a geostrophic wind normal to the leg of 2.9 m s^{-1}. Actual winds along the leg (Fig. 11b) averaged 2.7 m s^{-1} from about 112°. Since the track was along a 250°/160° heading, the component of the wind along the axis of the track of about 2.5 m s^{-1} was greater than the leg-normal component of the wind of 1.3 m s^{-1}. This suggests that the flow was directed with a component directed across the height contours toward lower heights, implying that the flow was accelerating as seen with leg C–D. Observer notes indicate that the Catalina eddy circulation terminated at the extreme western edge of this leg. This can be seen in the wind directions shown in Fig. 11b that reveal an abrupt transition from terrain-following easterly to southerly winds. Little variation in temperature and dewpoint temperature (Fig. 11c) was seen along leg E–F.

A vertical sawtooth pattern was then conducted between points E and F to sample the cloud layer and thermodynamic structure of the eddy circulation to the north of Santa Catalina Island. Unlike leg C–D only one sawtooth leg was conducted. Results (Fig. 12) show that the cloud-top height does not display the slope that is obvious in the previous sawtooth leg but rather appears fairly uniform. Cloud top is consistent with the trend of the isentropic surfaces that also are more uniform than that seen in legs farther to the south as in Fig. 8. Winds are less than 5 m s^{-1} throughout the sawtooth with a

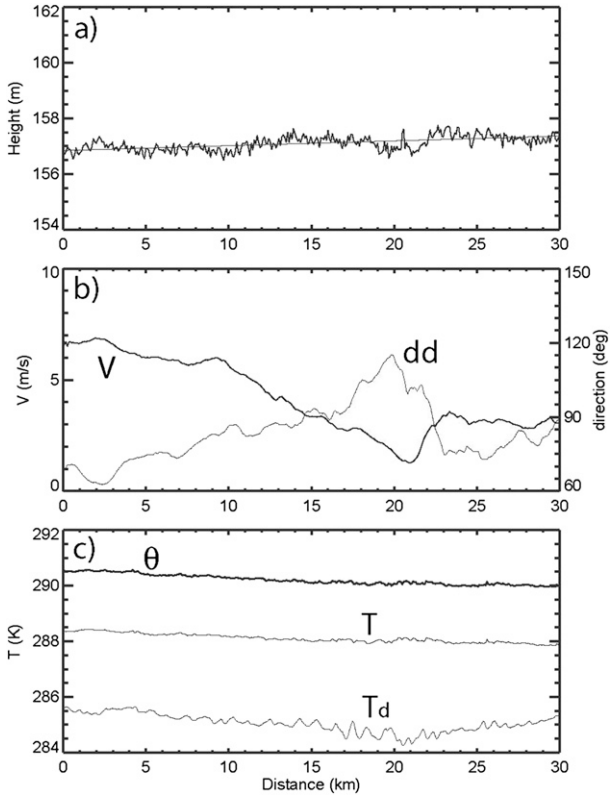

FIG. 13. As in Fig. 6, but for leg F–G at 1709–1716 UTC. North is to left.

slight decrease in wind speed of about $1\,m\,s^{-1}$ or so with winds decreasing away from the coast. Wind directions (not shown) remain constant throughout the sawtooth and are from roughly 135°, except at the western edge where southerly to southwest winds become established as the leg passes through the Catalina eddy circulation boundary. By 1700 UTC the cloud layer had become less defined, especially near the western edge of the sawtooth. In part this was thought to reflect the general solar heating and decrease in the eddy circulation.

A final isobaric leg was conducted between points F and G again about 150 m above the ocean, oriented with a heading of about 10°. The purpose of the leg was to again evaluate the PGF in the north–south direction. As was done with the initial leg, horizontal pressure changes were evaluated at nearby buoy sites. Pressures at NTBC1 and ICAC1 indicated pressures fluctuated by ±0.1 hPa during the flight leg; no height corrections were necessary to the isobaric heights. Figure 13 illustrates the UWKA observations during that final isobaric leg. Heights (Fig. 13a) show that the pressure gradient force remains directed from south to north and is comparable to leg A–B at the start of the flight. Support for the northward movement of the cloud layer is still present. Wind directions (Fig. 13b) indicate terrain influence with directions easterly for the first half of the leg that may reflect influence of the local terrain near Long Beach. As the UWKA approaches the coastal stretch near Point Mugu, wind shifts to a southeast direction that again follows the general coastline. The temperature field (Fig. 13c) is uniform showing only a slight increase toward the coast that is consistent with the sea surface temperatures (not shown) that are about 0.5°C warmer adjacent to the coast. Prior to landing at Point Mugu, a sounding was conducted just offshore that shows cloud base and top at about 600 and 850 m, respectively, similar to that experienced during the climbout.

4. Summary

Catalina eddies have been the topic of numerous studies in the past several decades. Some key conclusions reached as part of previous studies include the importance of leeside troughing as a result of downslope wind over the San Rafael and Santa Ynez mountains and damming of air by the coastal mountains to the south of Los Angeles. Such processes modify the horizontal pressure field such that lower pressures are found in the northern portion of the marine layer within the California Bight and support a thickening of the marine stratus along the coast and northward movement of the cloud layer. It was observed during PreAMBLE that cyclonic vorticity was a ubiquitous feature of the lower marine atmosphere within the California Bight; eddy circulations were observed during the morning hours on 24 of the 33 days during which PreAMBLE field operations were conducted. This is consistent with the mean June 2008 climatology based on the Advanced Research Weather Research and Forecasting Model (ARW-WRF) simulations that showed cyclonic vorticity within the California Bight was present. In this sense, eddy circulations owe their existence to the orientation of the Southern California coastline as suggested by Wakimoto (1987) and Thompson et al. (1997).

Airborne observations from the UWKA missions conducted during PreAMBLE provide some of the most detailed measurements regarding the dynamics of the Catalina eddy, especially for the 9 June 2012 case. As noted from previous work (e.g., Mass and Albright 1989), the best cases of Catalina eddy formation occurred during episodes of strong northerly flow west of Point Conception including the 9 June 2012 case. Little evidence was seen of leeside troughing in setting up lower pressures along the northern coastline of the California Bight for this case, despite the persistence of strong northerly winds over the ocean to the west. The

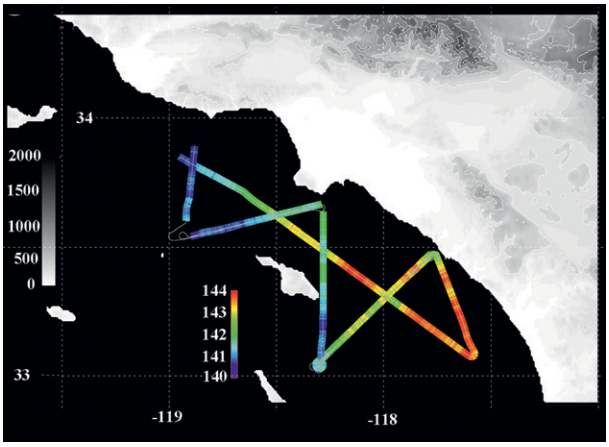

FIG. 14. Color-coded heights (m) of the 994.8-hPa isobaric surface with isallobaric corrections included of all UWKA isobaric legs conducted during the 9 Jun 2012 flight. Topography (m) is gray shaded.

horizontal pressure field as determined from GPS analyses revealed that pressure was lower from the Santa Barbara Channel eastward to at least Long Beach than the pressure south of Santa Catalina Island. A northward-directed PGF along the eastern side of the California Bight persisted throughout most of the day on 9 June 2012 and reflected the larger-scale pressure field, established as a result of land–ocean contrast. A summary of the heights is shown in Fig. 14. Here all isobaric legs have been corrected to a common 994.8-hPa surface and isallobaric corrections applied as discussed previously. Subtle gradients in the height field can be detected. Two primary signals can be identified. First, heights rise from north–south along the initial long flight leg. Second, blocking by the coastal terrain is present as indicated by heights increasing toward the coastline. This suggests that a net northward acceleration exists along the eastern edge of the California Bight and the cloud motion depicted on satellite imagery is consistent with these measurements.

Other case studies from PreAMBLE showed that lower pressures were consistently seen over the warm continent along the entire California coast. In this manner it is suggested that supporting horizontal pressure gradients need not be the result of special atmospheric conditions but rather are nearly ubiquitous. Such meridional signals are weak, roughly 2 m or a 0.25-hPa pressure difference over the 150-km leg for the 9 June 2012 case, yet are sufficient to promote the northward expansion of the cloud layer. Evidence of blocking by the coastal mountains was present during the 9 June 2012 case, especially south of Los Angeles. Cloud tops of the marine stratus were approximately 150 m higher at the coast as compared to 60 km farther west. Measured coast-normal pressure gradient forces are also subtle, similar in magnitude to the north–south gradient. From measurements of the horizontal pressure field, flows associated with the Catalina eddy are quasigeostrophic but with detectable accelerations northward. Such measurements confirm that the movement of such a cloud layer is similar to that observed during conditions of a coastally trapped wind reversal such as suggested by Skamarock et al. (2002).

Acknowledgments. This research was supported in part by the National Science Foundation through Grant AGS-1034862. The authors wish to thank pilots Ahmad Bandini and Brett Wadsworth and scientists Jeff French and Larry Oolman for help with the PreAMBLE field study and UWKA measurements.

REFERENCES

Beardsley, R. C., C. E. Dorman, C. A. Friehe, L. K. Rosenfeld, and C. D. Winant, 1987: Local atmospheric forcing during the Coastal Ocean Dynamics Experiment 1. A description of the marine boundary layer and atmospheric conditions over a northern California upwelling region. *J. Geophys. Res.,* **92** (C2), 1467–1488.

Bosart, L. F., 1983: Analysis of a California Catalina eddy. *Mon. Wea. Rev.,* **111,** 1619–1633.

Burk, S. D., and W. T. Thompson, 1996: The summertime low-level jet and marine boundary layer structure along the California coast. *Mon. Wea. Rev.,* **124,** 668–686.

Clark, J. H. E., and S. R. Dembek, 1991: The Catalina eddy event of July 1987: A coastally trapped mesoscale response to synoptic forcing. *Mon. Wea. Rev.,* **119,** 1714–1735.

Davis, C., S. Low-Nam, and C. Mass, 2000: Dynamics of a Catalina eddy revealed by numerical simulation. *Mon. Wea. Rev.,* **128,** 2885–2904.

Dorman, C. E., 1985: Evidence of Kelvin waves in California's marine layer and related eddy generation. *Mon. Wea. Rev.,* **113,** 827–839.

——, and C. D. Winant, 2000: The marine layer in and around the Santa Barbara Channel. *Mon. Wea. Rev.,* **128,** 261–282.

——, and D. Koračin, 2008: Response of the summer marine layer flow to an extreme California coastal bend. *Mon. Wea. Rev.,* **136,** 2894–2922.

Koračin, D., and C. E. Dorman, 2001: Marine atmospheric boundary divergence and clouds along California in June 1996. *Mon. Wea. Rev.,* **129,** 2040–2056.

Mass, C. F., and M. D. Albright, 1987: Coastal southerlies and alongshore surges of the west coast of North America: Evidence of mesoscale topographically trapped response to synoptic forcing. *Mon. Wea. Rev.,* **115,** 1707–1738.

——, and ——, 1989: Origin of the Catalina eddy. *Mon. Wea. Rev.,* **117,** 2406–2436.

Nuss, W. A., and Coauthors, 2000: Coastally trapped wind reversals: Progress toward understanding. *Bull. Amer. Meteor. Soc.,* **81,** 719–743.

Parish, T. R., and D. Leon, 2013: Measurement of cloud perturbation pressures using an instrumented aircraft. *J. Atmos. Oceanic Technol.,* **30,** 215–229.

——, M. D. Burkhart, and A. R. Rodi, 2007: Determination of the horizontal pressure gradient force using global positioning system on board an instrumented aircraft. *J. Atmos. Oceanic Technol.,* **24,** 521–528.

——, D. A. Rahn, and D. Leon, 2008: Aircraft observations of a coastally trapped wind reversal off the California coast. *Mon. Wea. Rev.,* **136,** 644–662.

Pomeroy, K. R., and T. R. Parish, 2001: A case study of the interaction of the summertime coastal jet with the California topography. *Mon. Wea. Rev.,* **129,** 530–539.

Rahn, D. A., and T. R. Parish, 2007: Diagnosis of the forcing and structure of the coastal jet near Cape Mendocino using in situ observations and numerical simulations. *J. Appl. Meteor. Climatol.,* **46,** 1455–1468.

——, and ——, 2008: A study of the forcing of the 22–25 June 2006 coastally trapped wind reversal based on numerical simulations and aircraft observations. *Mon. Wea. Rev.,* **136,** 4687–4708.

Rosenthal, J., 1968: Picture of the month: A Catalina eddy. *Mon. Wea. Rev.,* **96,** 742–743.

Saha, S., and Coauthors, 2010: The NCEP Climate Forecast System Reanalysis. *Bull. Amer. Meteor. Soc.,* **91,** 1015–1057.

Schwerdtfeger, W., 1975: The effect of the Antarctic Peninsula on the temperature regime of the Weddell Sea. *Mon. Wea. Rev.,* **103,** 45–51.

Skamarock, W. C., R. Rotunno, and J. B. Klemp, 2002: Catalina eddies and coastally trapped disturbances. *J. Atmos. Sci.,* **59,** 2270–2278.

Thompson, W. T., S. D. Burk, and J. Rosenthal, 1997: An investigation of the Catalina eddy. *Mon. Wea. Rev.,* **125,** 1135–1146.

Ueyoshi, K., and J. O. Roads, 1993: Simulation and prediction of the Catalina eddy. *Mon. Wea. Rev.,* **121,** 2975–3000.

Ulrickson, B. L., J. S. Hoffmaster, J. Robinson, and D. Vimont, 1995: A numerical modeling study of the Catalina eddy. *Mon. Wea. Rev.,* **123,** 1364–1373.

Wakimoto, R., 1987: The Catalina eddy and its effect on pollution in Southern California. *Mon. Wea. Rev.,* **115,** 837–855.

Wang, Z., P. Wechsler, W. Kuestner, J. French, A. R. Rodi, B. Glover, M. Burkhart, and D. Lukens, 2009: Wyoming Cloud Lidar: Instrument description and applications. *Opt. Express,* **17,** 13 576–13 587.

——, J. French, G. Vali, and P. Wechsler, 2012: Single aircraft integration of remote sensing and in situ sampling for the study of cloud microphysics and dynamics. *Bull. Amer. Meteor. Soc.,* **93,** 653–668.

Zemba, J., and C. A. Friehe, 1987: The marine boundary layer jet in the Coastal Ocean Dynamics Experiment. *J. Geophys. Res.,* **92** (C2), 1489–1496.